APS European Society for Paediatric Research SPR Society for Pediatric Research

BASIC SCIENCE ARTICLE

Check for updates

Maternal immune activation alters fetal and neonatal microglia phenotype and disrupts neurogenesis in mice

Marco Loayza[1], Shuying Lin[2], Kathleen Carter[1], Norma Ojeda[1], Lir-Wan Fan[1], Sumana Ramarao[1], Abhay Bhatt[1]✉ and Yi Pang[1]✉

BACKGROUND: Activation of microglia, increase in cortical neuron density, and reduction in GABAergic interneurons are some of the key findings in postmortem autism spectrum disorders (ASD) subjects. The aim of this study was to investigate how maternal immune activation (MIA) programs microglial phenotypes and abnormal neurogenesis in offspring mice.

METHODS: MIA was induced by injection of lipopolysaccharide (LPS, i.p.) to pregnant mice at embryonic (E) day 12.5. Microglial phenotypes and neurogenesis were investigated between E15.5 to postnatal (P) day 21 by immunohistochemistry, flow cytometry, and cytokine array.

RESULTS: MIA led to a robust increase in fetal and neonatal microglia in neurogenic regions. Homeostatic E15.5 and P4 microglia are heterogeneous, consisting of M1 (CD86+/CD206−) and mixed M1/M2 (CD86+/CD206+)-like subpopulations. MIA significantly reduced M1 but increased mixed M1/M2 microglia, which was associated with upregulation of numerous cytokines with pleotropic property. MIA resulted in a robust increase in Ki67+/Nestin+ and Tbr2+ neural progenitor cells in the subventricular zone (SVZ) of newborn mice. At juvenile stage, a male-specific reduction of Parvalbumin+ but increase in Reelin+ interneurons in the medial prefrontal cortex was found in MIA offspring mice.

CONCLUSIONS: MIA programs microglia towards a pleotropic phenotype that may drive excessive neurogenesis in ASD patients.

Pediatric Research (2023) 93:1216–1225; https://doi.org/10.1038/s41390-022-02239-w

IMPACT:

- Maternal immune activation (MIA) alters microglial phenotypes in the brain of fetal and neonatal mouse offspring.
- MIA leads to excessive proliferation and overproduction of neural progenitors in the subventricular zone (SVZ).
- MIA reduces parvalbumin+ while increases Reelin+ interneurons in the prefrontal cortex.
- Our study sheds light on neurobiological mechanisms of abnormal neurogenesis in certain neurodevelopmental disorders, such as autism spectrum disorder (ASD).

INTRODUCTION

Maternal infection is a well-recognized risk factor for a broad range of neurodevelopmental disorders (NDDs), including brain white matter injury, bipolar disorder, schizophrenia, and autism spectrum disorders (ASD).[1–3] A large body of research has demonstrated that the timing of infection is a critical factor in determining neurobiological and behavioral phenotypes in affected offspring. Specifically, infection at early to mid-gestation, a developmental period of active neurogenesis, is associated with higher incidences of ASD and schizophrenia, whereas infection at late gestation is typically associated with cerebral palsy and brain white matter injury.[3,4] The pathogenic role of maternal infection in ASD and schizophrenia has been extensively investigated using the maternal immune activation (MIA) animal models, typically by treating pregnant animals with endotoxin lipopolysaccharide (LPS) or viral mimic double strand RNA polyinosinic:polycytidylic acide (poly (I:C)). For instance, MIA at early to mid-gestation, typically between embryonic (E) 9 to 15, is sufficient to trigger ASD-like behaviors in rodent offspring.[5–7] However, the neurobiological mechanisms underpinning ASD-like behavioral deficits are largely unknown. Additionally, most of the assessments were performed at late postnatal ages while limited data are available for the fetal and/or newborn period.[8]

Converging evidence suggests that in ASD and schizophrenia subjects, altered neurodevelopmental trajectory starts early in development, most likely at embryonic or early fetal stage. This is a critical period of neurogenesis, when neural stem cells (NSCs) and neural progenitor cells (NPCs) undergo rapid proliferation, migration, differentiation, and target selection. Although ASD is considered a disorder of brain connectivity rooted in faulty synaptic development, recent studies suggest that dysregulation in neurogenesis likely plays a significant role.[9,10] For instance, several postmortem studies reported increased cortical neuron density and disorganization of cortical cytoarchitecture in 2–16-year-old ASD children, while anatomical and neuroimaging studies consistently reported increased whole brain volume or head

[1]Department of Pediatrics, University of Mississippi Medical Center, Jackson, MS 39216, USA. [2]Department of Physical Therapy, University of Mississippi Medical Center, Jackson, MS 39216, USA. ✉email: abhatt@umc.edu; ypang@umc.edu

Received: 11 March 2022 Revised: 12 June 2022 Accepted: 22 July 2022
Published online: 13 August 2022

circumference in a subset of ASD individuals at early ages.[11–14] Collectively, these findings suggest the possibility that neurogenesis is accelerated during a specific window of early development. Experimental studies supporting this hypothesis include findings that NPCs derived from inducible plural stem cells (iPSCs) of living ASD subjects exhibit accelerated proliferation potentials,[15] and maternal LPS or poly (I:C) exposure leads to enhanced proliferation of NSCs in mice offspring.[16,17]

Microglia, which are the resident immune cells of the brain, play a pivotal role in regulating neuronal numbers through phagocytosis and secreted cytokines during development. In the mature brain, activated microglia exhibit either proinflammatory or anti-inflammatory phenotypes that have distinct functional impact on neurons.[18,19] However, whether fetal microglia behave similarly from their adult counterparts, in terms of phenotypes and functional impact on neurogenesis, is entirely unclear. Therefore, the aim of this study was to assess microglial phenotypes and neurogenesis in MIA-exposed offspring at both fetal and neonatal period.

EXPERIMENTAL PROCEDURES

Animals and treatments

This study was conducted in strict accordance with the National Institutes of Health Guide for the Care and Use of Laboratory Animals. The animal protocol for the study was approved by the Institutional Animal Care and Use Committee at the University of Mississippi Medical Center. All efforts were made to minimize the discomfort and stress of animals. Eight-week old male and female C57BL/6J mice were purchased from Jackson Laboratory (Bar Harbor, ME). Mice were group housed 3–4 per cage on a 12 h light/12 h dark cycle in a temperature- and humidity-controlled environment, with water and food provided ad libitum. Mice were acclimated to the laboratory facility for two weeks before breeding at 10 weeks old.

For time pregnancy, the day of vaginal plug detection was designated as embryonic (E) day 0.5. On E12.5, dams were injected with LPS (50 µg/kg body weight, intraperitoneal) or sterile saline as controls. All injections were performed at 4 PM local time. Body weight was recorded daily at 9 AM. E12.5 in mice corresponds to early gestation in humans, a developmental period that is associated with increased risk of ASD upon maternal infections.[3,4] In this study, the litter was considered the experimental unit. For a balanced experimental design, individual offspring within a litter was assigned to different experiments or the same experiment at different time points.

Reagents

Unless otherwise stated, all chemicals used in this study were purchased from Sigma (St. Louis, MO). Details of antibodies are listed in Table 1.

Immunohistochemistry

Dams (for E15.5 fetuses) or postnatal (P) day 1 and 21 offspring were perfused transcardially with saline followed by 4% paraformaldehyde (PFA). Brains were post-fixed for additional 24 h and then immersed in cytoprotection solutions (sequentially in 10%, 20%, and 30% sucrose, each for 24 h). Serial frozen free-floating coronal sections (45 µm) were prepared using a freezing microtome (Leica, SM 2000R, Wetzlar, Germany). For immunofluorescence staining of Ki67 and Tbr2, antigen retrieval protocol was applied based on pilot experiments. Briefly, sections were rinsed in phosphate-buffered saline (PBS) and transferred to a 50 ml conical tube containing citrate buffer (pH 6.0). Sections were heated to 85 °C for 20 min in a water bath. Sections were cooled to room temperature (RT), washed with PBS, and blocked with 10% normal goat serum (Millipore, Billerica, MA) in PBS for 1 h at RT. Sections were then incubated with primary antibodies overnight at 4 °C with gentle shaking. The next day, sections were washed three times in PBS and incubated with secondary antibodies conjugated with Alexa fluor 488 (1:400) or 555 (1:2000) at RT for 1.5 h. Following washing in PBS, sections were mounted on slides and air-dried. DAPI (100 nM) was included in the mounting medium for counter-staining.

Stereological cell counting

All cell counting was conducted based on design-based stereological principal by the Stereo Investigator software package (MBF Bioscience, Williston, VT), as described previously.[20] Image stacks were acquired using a cooled monochrome camera coupled to a motorized fluorescence microscope (Nikon Nie, NY). Iba1+ microglia, Ki67+ mitotic cells, and TBR2+ intermediate NPCs were counted in the subventricular zone (SVZ) of 3 coronal sections (prepared as in 1 in 6 series) at the level of the frontal cortex. The contour of SVZ was outlined using a ×2.5 objective lens. A systemic random grid was placed on the outlined contour, and image stacks were acquired using a ×60 oil objective lens. Immunopositive cells were counted using the optical fractionator probe. Due to the small area of SVZ, positive cells were counted exhaustively using larger counting frames (150 µm × 110 µm) within smaller systematical random sampling grids (160 µm × 120 µm). Probe depth was set at 18 µm with 2 µm guard zones on each side of the section. Iba1+ cell counting was presented as cell density (numbers of cells/mm^3). Due to apparently larger areas occupied by Ki67 and Tbr2+ cells in LPS treated compared to the control mice, they were presented as total number of cells.

The number of Parvalbumin (PV)+ and Reelin+ neurons was counted within the medial prefrontal cortex (mPFC) in nine double-immunostained serial sections. Delineating the boundary of mPFC was in accordance with the published protocol for adult mice brain.[21] The systematic random grid size was set at 250 × 200 µm while other parameters were the same as above. Image stacks containing PV+ (FITC channel), Reelin+ (TRITC

Table 1. Antibodies used in in this study.

Antibody name	Source	Catalog number	Dilution	Application
CD11b	ThermoFisher	501123703	100	FACS
CD45	ThermoFisher	5014971	100	FACS
CD206	ThermoFisher	12206182	200	FACS
CD86	ThermoFisher	501129188	200	FACS
Iba1	Wako	01919741	1000	IHC
Ki67	ThermoFisher	14569882	500	IHC
Nestin	Santa Cruz	Sc-20978	500	IHC
Tbr2	Abcam	Ab23345	600	IHC
Parvalbumin	Abcam	Ab11427	500	IHC
Reelin	Millipore	Mab5364	500	IHC

channel), and total cells (DAPI channel) were acquired under a ×60 oil objective lens. Total cell number within the entire mPFC was calculated by the Stereo Investigator software.

Flow cytometry (fluorescence-activated cell sorting (FACS))

On E15.5 and P4, mice were rapidly perfused intracardially with ice-cold PBS. The forebrain of fetal or neonatal mice were dissected on ice under a stereoscope. The meninges were carefully removed and forebrain tissue was dissociated into single cell suspension using the Neural Tissue Dissociation Kit P (Miltenyi Biotec), following the manufacturer's instruction. The dissociated cells were resuspended in 1 × HBSS and passed through a 45 µm strainer to remove any clusters of cells or tissue debris. Total number of live cells was estimated using a hemocytometer. For FACS, 2×10^6 cells in 100 µl FACS buffer (PBS containing 1% bovine serum albumin) were first stained with Live/Dead kit (Miltenyi Biotec) on ice for 10 min. Following washing in FACS buffer, cells were pelleted by centrifugation at 300 × *g* for 5 min. Cells were resuspended in FACS buffer and blocked with FC-receptor blocker CD16 antibody (BD Bioscience) for 10 min on ice, and incubated with the following primary antibodies conjugated with various fluorochromes at 4 °C for 30 min: CD45-APC, CD11b-PerCP-Cy5.5, CD206-PE, and CD86-PE-Cy7. FACS analysis was performed using a Beckman Coulter Gallios Analyzer (Beckman). Viable cells were gated under FITC channel, and microglial population were gated as CD11b+/CD45^{intermediate}. CD86 and CD206 were used as surface markers to identify M1- and M2-like microglia, respectively.[22] We found that CD86 is constitutively expressed by microglia, independent of the ages of animals (i.e., E15.5 and P4) or experimental conditions (i.e., SA vs LPS), while CD206 expression is affected by both the age and LPS treatment, leaving the majority of microglia falling into either CD86+/CD206− (defined as M1) or CD86+/CD206+ (defined as mixed M1/M2) subpopulations. Therefore, their relative abundance was calculated as a percentage to total microglia (CD11b+/CD45^{intermediate}).

Cytokine array

Profiling of 96 cytokines in acutely isolated microglia was conducted using membrane-based cytokine array kits (Cat#AAM-CYT-1000, RayBiotech). To prepare enough cells for a single array, all fetuses (E15.5) or pus (P4) within a single litter of control or MIA were combined as a single sample. Microglia were isolated from E15.5 and P4 mouse brain as described above. Total protein lysis was prepared immediately upon cell isolation. Briefly, cells were suspended in 0.8 ml cell lysis buffer (ThermoFisher Scientific, MA) and homogenized using an ultrasonic sonicator (Qsonicas, LLC, CT), and centrifuged at 12,000 × *g* for 10 min. The supernatant was collected and total protein was determined by BCA method. Samples that contain 400 µg total protein were used for cytokine array. Chemiluminescence signals were acquired by the ChemiDoc MP imaging system (Bio-Rad, CA). An excel-based software supplied by the vendor (RayBiotech) was used to analyze the array data. The optical density of target cytokines (minus background) was normalized to positive controls. Since this approach was aimed at profiling differentially expressed cytokines from different classes (e.g., proinflammatory vs anti-inflammatory) rather than quantifying individual cytokine expression levels, only one dam for each group was used ($N = 1$ in Table 2). To increase robustness of this approach, cytokine array was repeated once (using the same microglial lysis) and the values of individual cytokines were averaged from these two independent arrays. A 1.5-fold change (increase or decrease) in cytokine levels is considered significant.

Data analysis

Data were analyzed by unpaired *t* test (E15.5 and P1) or two-way analysis of variance (P21) followed by post hoc Tukey test using the SigmaPlot software (version 11). Data are presented as mean ± SEM. A value of $p < 0.05$ was considered statistically significant.

Table 2. Upregulated cytokines in E15.5 microglia upon MIA.

Cytokine name	Fold change
CD27	1.7
CD27L	1.7
CD30	1.7
CD30L	1.6
CD36/SR-B3	1.7
Cytotoxic T-lymphocyte protein 4 (CTLA-4)	1.5
CXCL16	1.5
Decorin	1.5
Dickkopf-related protein 1 (DKK1)	1.5

Cytokine levels in acutely isolated microglia were compared between MIA and controls by cytokine array detecting 96 cytokines. A single litter (combined all littermates to prepare enough microglia) in each group was used for this study. Values represent fold changes (MIA over control) and a 1.5-fold increase or decrease is considered significant.

RESULTS

MIA leads to a robust activation of fetal microglia that persists into early postnatal age

We first sought to evaluate overall response of microglia upon maternal LPS challenge by assessing changes of Iba1+ microglial density, morphology, and regional distribution by immunohistochemistry. At E15.5, Iba1+ microglia were highly concentrated in the periventricular regions. Maternal LPS led to a dramatic change of microglia morphology, characterized by intense Iba1 immunostaining, enlarged soma sizes, and retraction of processes (Fig. 1d). At P1, a robust increase of Iba1+ cells was readily observed under low magnifications (Fig. 1f, g). The increase was most noticeable in the hippocampus and subventricular zone (SVZ) (Fig. 1f–k), and to a lesser extent, basal forebrain structures such as the thalamus and basal ganglia. Due to a much lower density of Iba1+ cells in the control compared to MIA, the cerebral cortex appeared to be the least affected region (Fig. 1g). Stereological counting showed that the density of Iba1+ cells in the SVZ was more than doubled in LPS group compared to the control at P1 (SA: 5.52 ± 0.53, LPS: 11.28 ± 0.72, $p < 0.001$).

MIA drives fetal and neonatal microglia towards CD86+/CD206+ phenotype

Next, we conducted flow cytometry experiments to assess microglia phenotypes using CD86 and CD206, two well-established markers for proinflammatory M1-like or anti-inflammatory M2-like states. Microglia were distinguished from macrophages based on CD45 expression: microglia express intermediate while macrophages express high levels of CD45. Therefore, we first gated CD11b+/CD45^{intermediate} microglia from total neural cells, and then analyzed CD86+ and CD206+ microglia (Fig. 2a). We identified two microglial subgroups in the E15.5 control mice based on CD86 and CD206 expression levels: CD86+/CD206− (M1-like) and CD86+/CD206+ (mixed M1/M2-like) cells, which accounted for 31.1% and 54.6% of total microglia, respectively. MIA led to a significant decrease of CD86+/CD206− while simultaneous increase of CD86+/CD206+ cells (Fig. 2b, c). In addition, within the CD86+/CD206+ microglia population, a new subgroup of CD86+/CD206^{high} cells were clearly visible in the MIA mice brain (circled in the right panel of Fig. 2b), which was not observed in the control. At P4, CD86+/CD206− and CD86+/CD206+cells accounted for 8.5% and 72.6% of total microglia in the control mice, indicating an increase of CD206 expression on microglia during normal fetal to early postnatal

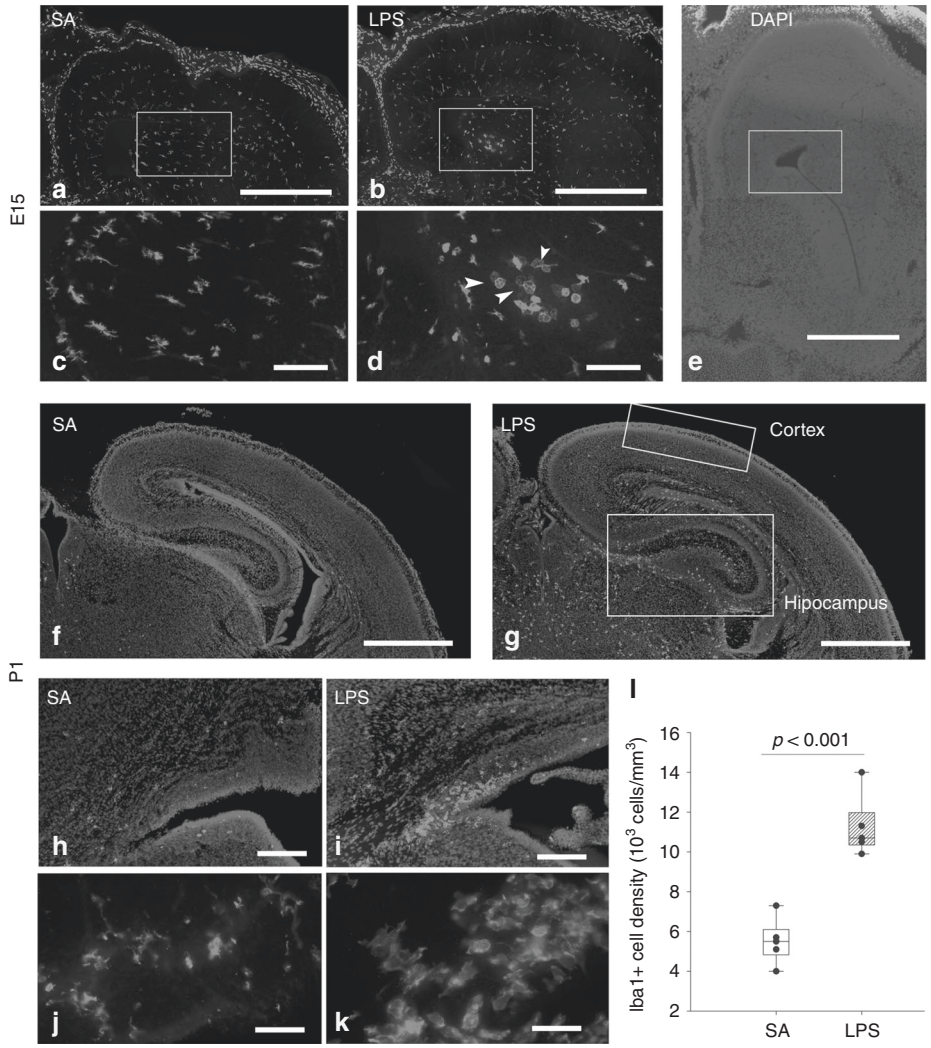

Fig. 1 MIA leads a robust activation of microglia in the brains of E15.5 and P1 offspring. Representative micrographs show the distribution of Iba1+ cells in the E15.5 (**a**–**e**) and P1 (**f**–**k**) mouse brains following MIA. At E15.5, morphological transformation of microglia in the periventricular area (white boxes in **a**, **b**) of MIA mice was evident by their larger soma sizes and retracted processes. Some "grape-like" Iba1+ cells that contain multiple nuclei were noted in MIA mice (arrowheads in **d**). The anatomical landmark of the corresponding brain sections in (**a**, **b**) is depicted in **e**. At P1, a dramatic increase of Iba1+ microglia was clearly visible in brains from MIA mice, especially the hippocampus (**f**, **g**) and the SVZ (**h**–**k**). Stereological counting shows a more than two-fold increase of microglia density in the SVZ of MIA offspring (**l**). Scale bars: 1000 µm (**a**, **b**, **e**–**g**), 100 µm (H&I), 50 µm (**c**, **d**, **j**, **k**). $N = 5$ each group.

development. However, MIA significantly accelerated this change. The percentage of CD86+/CD206− cells was significantly reduced (2.7 ± 0.25 vs 8.5 ± 0.33%, $p < 0.001$) while that of CD86+/CD206+ cells was increased (72.6 ± 1.6 vs 88.0 ± 1.1%, $p < 0.001$) (Fig. 2d, e) as compared to the control.

MIA causes differential expression of cytokines by microglia

To gain further insight into potential functional implications of microglia phenotypes identified by FACS, we then compared cytokine expression profiles in acutely isolated E15.5 and P4 microglia from control and MIA offspring by cytokine array. Based on their functions, 94 target cytokines could be divided broadly into four categories: inflammatory cytokines and their receptors, chemokines, growth factors, and extracellular matrix proteins. We identified 9 and 14 cytokines that were upregulated by MIA on E15.5 and P4, respectively (Tables 2 and 3). Interestingly, a number of upregulated cytokines at E15.5 are not inflammatory in nature but rather related to microglial phagocytosis (CD36, CXCL16, Decorin, and LTLA-4), while several upregulated cytokines at P4 belong to Th17 inflammatory response (IL-17A, IL-17E, and IL-17 receptor B). It is worth noting that Osteopontin was consistently higher in microglia from MIA offspring on both E1.5 (1.4-fold) and P4 (1.5-fold), but since 1.5-fold change was used as the cutoff value, Osteopontin is only listed on P4 in Table 2.

MIA leads to enhanced proliferation and overproduction of NPCs in the SVZ

Although CD206+ microglia are generally considered anti-inflammatory and neurotrophic (so called M2-like microglia) in neurodegenerative disorders, it remains unclear whether they have similar functions in NDDs. To test whether this type of microglial activation is associated with a pleotropic effect on neurogenesis, we first quantified cell proliferation by Ki67 immunofluoresence in the P1 offspring. As demonstrated in Fig. 3, MIA led to a massive increase in Ki67+ cells that mainly located in the SVZ. Given LPS could stimulate microglia proliferation in vivo,[23] we then examine whether some of the Ki67+ cells were microglia. Double immunofluoresence revealed that in the SVZ at the frontal cortex level, very few Iba1+ cells were co-labeled with Ki67. Instead, the vast majority of Ki67+ cells were

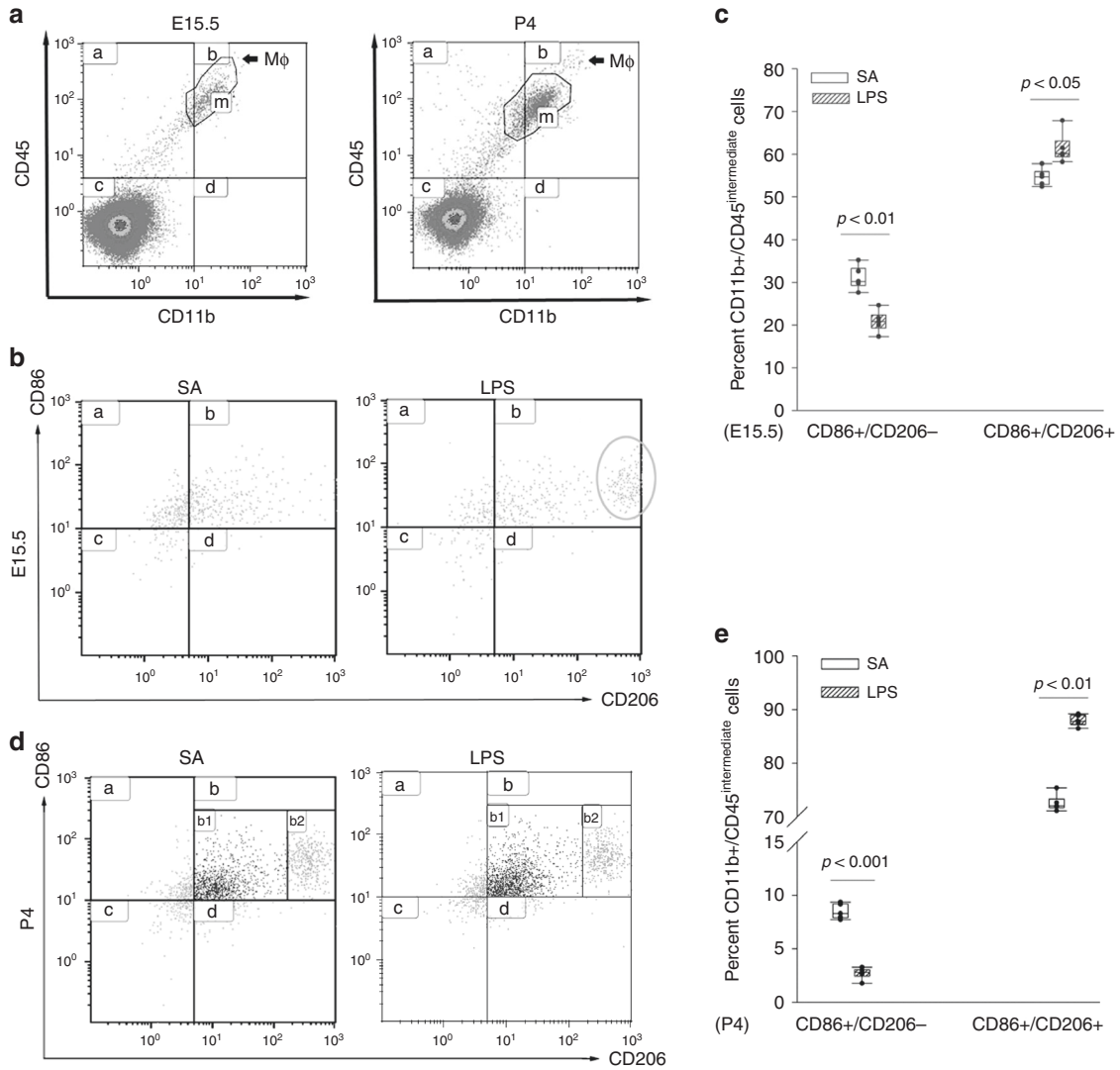

Fig. 2 Flow cytometry analysis of microglia phenotypes. Microglia were gated as CD11b+/CD45^{intermediate} cells (outlined as m for E15.5 and P4) from total neural cells, while macrophages were identified as CD45+/CD45^{high} fractions (Mφ) (**a**). MIA resulted in a significant decrease of CD86+/CD206− while increase in CD86+/CD206+ microglia populations in the E15.5 fetal brain (**b**, **c**). A distinct CD86+/CD206^{high} microglial subpopulation was observed in LPS-treated fetal brain (green circle in the right panel of **b**). Analysis of microglia phenotypes of P4 mice showed similar changes of CD86+/CD206− and CD86+/CD206+ microglia polarization (**d**, **e**). $N = 5$ each group.

positive for nestin, a marker for NSCs and/or NPCs, raising the question whether increased proliferation of NSCs/NPCs could lead to overproduction of neurons. Considering the NSC-derived intermediated Tbr2+ NPCs serve as transient amplifying progenitors for later born doublecortin (DCX)+ neuroblasts, which migrate to and populate the developing cortex, we quantified the number of Tbr2+ NPCs in the SVZ by stereology. We found that, indeed, the number of Tbr2+ NPCs was significantly higher in MIA offspring compared to the control (Fig. 4b, c).

MIA disrupts cortical GABAergic interneuron development

The above data suggest MIA disrupted development of cortical excitatory neurons. Next we investigated whether the development of inhibitory interneurons were also affected, considering reduction of PV+ and Reelin+ interneurons has been reported in human ASD subjects and animal models of ASD.[24] We performed double-immunofluorescence and determined the total number of PV+ and Reelin+ neurons in the mPFC of P21 male and female offspring by stereology. Our data showed that MIA led to a significantly reduction in total PV+ neurons (7244 ± 628 vs $10{,}391 \pm 497$, $p < 0.05$) but increase in Reelin+ neurons ($16{,}360 \pm 665$ vs $11{,}686 \pm 803$, $p < 0.001$) in male offspring. However, we did not found any differences in PV neurons ($10{,}197 \pm 1388$ vs 8988 ± 878, $p > 0.05$) and Reelin neurons ($14{,}262 \pm 841$ vs $13{,}553 \pm 1120$, $p > 0.05$) between MIA and control female offspring (Fig. 5).

DISCUSSION

NDDs such as ASD have a complex etiology that involves many genetic and environmental risk factors. Maternal infection is a well-recognized risk factor for not only ASD but also other NDDs such as schizophrenia, ADHD, encephalopathy of prematurity, etc., suggesting that disruptions in critical early neurodevelopmental programs by inflammatory pathways, such as neurogenesis, may serve as a shared mechanism across NDDs. A large body of studies has shown that microglia activation plays a pivotal role in the pathogenesis of ASD, but the underlying mechanisms are largely unknown. For the best of our knowledge, this is the first study demonstrating the existence of heterogeneous M1 and mixed M1/M2 subgroups of microglia in the early developing mouse brain. More importantly, MIA polarizes microglia towards lower M1 and

Table 3. Upregulated cytokines in P4 microglia upon MIA.

Cytokine name	Fold change
Fractalkine (CX3CL1)	2.2
Granzyme B	1.5
IL-13	1.5
IL-15	1.9
IL-17A	1.8
IL-17 receptor B	1.8
IL-17E	2.0
Osteopontin	1.5
Prolactin	1.5
Pro-MMP-9	1.7
Stem cell factor (SCF)	1.8
sTNFR1	1.7
sTNFR2	1.7
preprotachykinin-1 (TAC1)	1.7

Cytokine levels in acutely isolated microglia were compared between MIA and controls by cytokine array detecting 96 cytokines. A single litter (combined all littermates to prepare enough microglia) in each group was used for this study. Values represent fold changes (MIA over control) and a 1.5-fold increase or decrease is considered significant.

higher M1/M2-like state, which is associated with increased neurogenesis and dysregulated interneuron development.

Inflammatory cytokines from maternal or placental sources are considered as the main culprits in initiating fetal neuroinflammation and/or microglia activation in the MIA model. We previously reported that maternal LPS induces a rapid upregulation of TNFα, IL1β, and IL-6 mRNAs in the fetal rat brain.[25] Studies from other groups also found a widespread increase of TNFα+[26] and iNOS+ and IL1β+[27] microglia in the fetal brain upon maternal LPS challenge, suggesting that activated fetal microglia might be proinflammatory in nature. In terms of microglial morphology, studies are surprisingly limited with inconsistency. For example, Cunningham et al.[27] and Hsueh et al.[28] did not find any changes of Iba1+ microglial morphology upon maternal LPS challenge. However, O'Loughlin et al.[29] reported an increased percentage of amoeboid microglia and a decrease of ramified microglia in P7 and P40 (but not P14) mice offspring upon maternal LPS challenge. In the current study, we found that both the density and size of Iba1+ microglia were increased in E15.5 and P1 mouse brain upon MIA, especially in the neurogenic SVZ. Coincidently, we observed a robust increase in NSC proliferation in these regions, indicating that activated fetal microglia might be pleotropic in nature and drive this change. The concept of "M1- and M2-like" microglia is used to interpret deleterious vs beneficial effects of activated microglia in the context of neurological disorders. For example, CD206+ M2-like microglia were observed in the peri-infarct region at early phase of stroke,[30] while IGF-1 expressing microglia in the SVZ promote neurogenesis.[31] However, how microglia phenotypes are regulated in the MIA model and how they affect NSCs is poorly understood. Given fetal microglia develop rapidly in an evolving cellular environment, it is possible they respond to LPS differently from their adult counterparts.

In the current study, we found that morphological characteristics are poor indicators of functional states of activated microglia in the developing brain. Compared to mature microglia that exhibit typically "resting" or "ramified" morphology, the developing microglia resemble "reactive" mature microglia under pathological conditions, which exhibit larger soma and fewer, shorter processes. This may reflect their high activities in regulating neuronal development via secreted factors and phagocytosis. Upon MIA, the size and density of microglia were further increased. Assessment of microglia polarization by FACS indicates that activated microglia are not predominantly M1 or M2, but rather a mixed phenotype expressing both M1 and M2 markers. CD206 is a surface protein that plays an important role in microglial pinocytosis and phagocytosis.[32] We speculate that the shift towards predominantly CD86+/CD206^{intermediate} microglia may reflect a general increase of microglia phagocytosis, while the emergence of a small group of CD86+/CD206^{high} microglia represents an increase of region-specific microglia with high phagocytic activity. Indeed, we observed a small microglia population that exhibited multiple phagocytosed nuclei inclusions, specifically found in the neuroepithelium at the prefrontal cortex of both the E15.5 control and MIA; however, the number and size of those microglia, which were apparently engulfing surrounding cells (presumably NPCs), were much higher in the MIA group (Supplementary Fig. 1). Consistent with this notion, a number of upregulated cytokines at E15.5 are associated with macrophage/microglia phagocytosis. For example, CD36 plays an important role in macrophages/microglia-mediated myelin debris uptake in an experimental autoimmune encephalomyelitis (EAE) model.[33] The chemokine CXCL16, along with CD68 and class A macrophage SR (SR-A1/II), were expressed by foamy macrophages in the rim and by ramified microglia around chronic active lesions in the brain of multiple sclerosis patients, suggesting their involvement in myelin phagocytosis.[34] Decorin (also known as Biglycan), a leucine-rich proteoglycan that can bind to TLR4,[35] is upregulated in activated microglia induced by β-amyloid protein.[36] Osteopontin, which is upregulated by microglia upon hypoxia–ischemia/LPS treatment in mice,[37] is also expressed by infiltrating macrophages engulfing amyloid beta plaques.[38] In another EAE study, activated microglia and infiltrating macrophages showed upregulated expression of B7, the ligand of CTLA-4 that are expressed by T cells, while microglia also bound to CTLA-4 in vitro.[39] Interestingly, some of these cytokines such as CD30 are also expressed by non-microglial immune cells, or exist as extracellular matrix proteins (Decorin and osteopontin), raising the possibility that some of these cytokines might be phagocytized rather than synthesized by microglia. Indeed, CX3CL1, a chemokine produced by neurons to communicate with microglia via CX3CR1, was found more than 2-folds higher in microglia from MIA vs control mice. In addition, granzyme B and osteopontin, two important proteins participating in monocyte phagocytosis, were also upregulated in P4 microglia.

Several cytokines (IL13, IL15, IL17A, and IL17E) known to be produced mainly by Th17 leukocytes, were upregulated in microglia from MIA mice at P4. The IL-6–IL17A axis plays a critical role in MIA-associated ASD.[40] Although IL-17A can be detected in maternal blood, placenta, and fetal brain after MIA, the placenta is the main source of IL-6 and IL17A.[41] It is unclear whether those cytokines were synthesized by microglia or from other sources. It is quite unlikely that these cytokines were from contaminated leukocytes during cell separation process, as the purity of isolated microglia assessed by Iba1/CD11b double-immunofluorescence staining exceeded 99%. Nevertheless, we would like to acknowledge the limitation of cytokine data, since only one litter/sample (tissues from all littermates were combined for isolating microglia) per condition was used for the array.

We previously found that systemic LPS challenge at P3 results in upregulation of both pro- and anti-inflammatory markers in microglia, enhanced neurogenesis, and ASD-like behavioral deficits.[42] Studies from other groups demonstrated that not only proinflammatory cytokine IL1β, TNFα, and IL-6, but also anti-inflammatory cytokine IL-10 mRNAs were increased in the fetal brain following maternal LPS challenge.[29] Likewise, it was found that a range of pro- and anti-inflammatory cytokine proteins were upregulated in postnatal fetal serum and brains following maternal exposure to poly (I:C).[43] These studies suggest that

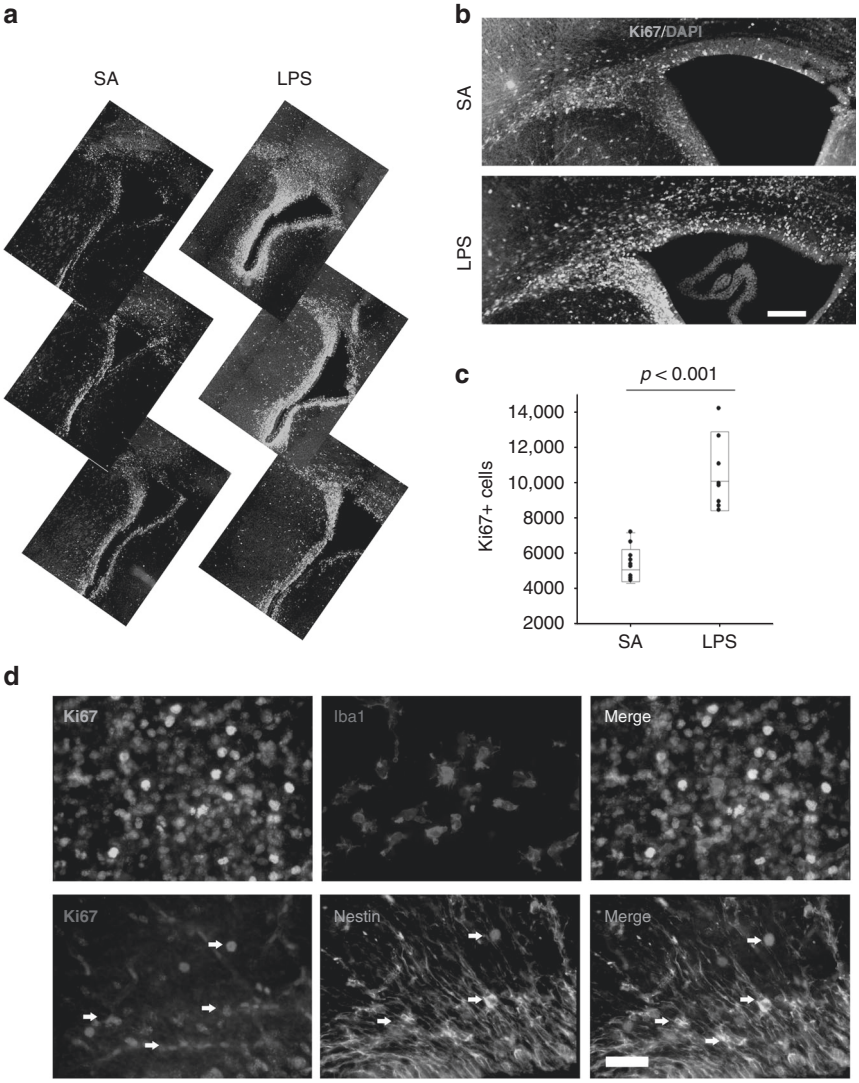

Fig. 3 MIA stimulates proliferation of NSCs in the offspring mouse brain. Representative serial micrographs at lower (**a**) and higher magnification (**b**) depict the distribution of Ki67+ cells in the SVZ at the level of frontal cortex of P1 mice. Stereological counting revealed a dramatic increase of Ki67+ cells in the SVZ of MIA vs control mice (**c**). Double immunofluorescence staining showed that the majority of Ki67+ cells were Nestin+ NSCs but not Iba1+ microglia (**d**). Scale bar: 100 µm (**b**), 50 µm (**d**). $N = 8$ per condition.

activated fetal microglia might be heterogeneous, consisting of both M1- and M2-like phenotypes. Our FACS data clearly showed that homeostatic fetal microglia are heterogeneous and express both M1- and M2-like markers, while MIA polarizes microglia towards predominantly mixed M1/M2-like phenotype. Interestingly, a transcriptomic study conducted using postmortem human brain tissue found that a cluster of microglial "M2-like" genes was significantly upregulated, which was correlated with a downregulated gene module involved in neurogenesis,[44] indicating that microglial polarization towards alternative or anti-inflammatory states may contribute to abnormal neurodevelopment in ASD.

Aberrant cytoarchitecture of the cerebral cortex and hippocampus were reported in several postmortem ASD studies as well as MIA animal models.[45] It is hypothesized that abnormal proliferation, differentiation, and migration of NPCs may contribute to these neuropathological observations. Again, there is discrepancy regarding effects of MIA on cell proliferation. For example, LPS exposure at E15–16 led to a reduction in Brdu+ cells in the DG of fetal and P14 mice[46] or rats,[47] while at E10.5 resulted in a significant decrease of neurogenesis in the DG of offspring at both P21 and P90.[48] Another study found that LPS at E9 did not affect DG neurogenesis at P21.[49] As mentioned earlier, the gestational age of MIA appears to be a critical factor accounting for differences in neurobiological and behavioral outcomes. Likewise, the time-sensitive nature of MIA in the etiology of NDDs is well recognized. Given rodents have a much shorter period of gestation than humans, variations in a few gestational days may have a considerable impact on MIA-mediated neurobiological response. In contrast to studies mentioned above, here we observed a robust increase of Ki67+ NSCs in the SVZ of P1 mice offspring, which is in agreement with recent studies demonstrating that maternal poly (I:C) enhanced NSC proliferation potentials[16] as well as increased Pax6+ and Tbr2+ NPCs in the fetal brain.[50] In addition, LPS treatment at E15 led to a significant increase in hippocampal pyramidal neuron spine density at P14.[7] All these evidence provides the notion that MIA may cause a pleotropic effect on NSCs/NPCs. The robust increase of Tbr2+ NPCs found in our MIA model suggests that some of the proliferating NSCs differentiated into TBr2+ intermediate progenitors. Although a few studies reported increase in cortical neurons of postmortem ASD subjects (2-16 years old), it is not

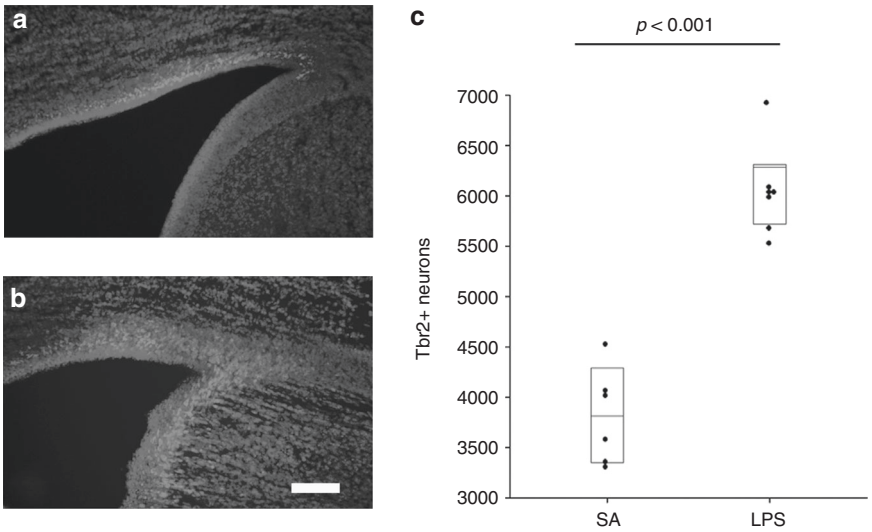

Fig. 4 Overproduction of Tbr2+ NPCs in the MIA offspring at P1. Representative immunostaining of Tbr2+ cells (red) in the SVZ of the control (**a**) and MIA mice (**b**). Stereological counting revealed a significant increase of Tbr2+ cells in the SVZ of MIA as compared to the control (**c**). Scale bars: 100 µm. $N = 6$ (SA) and 7 (LPS).

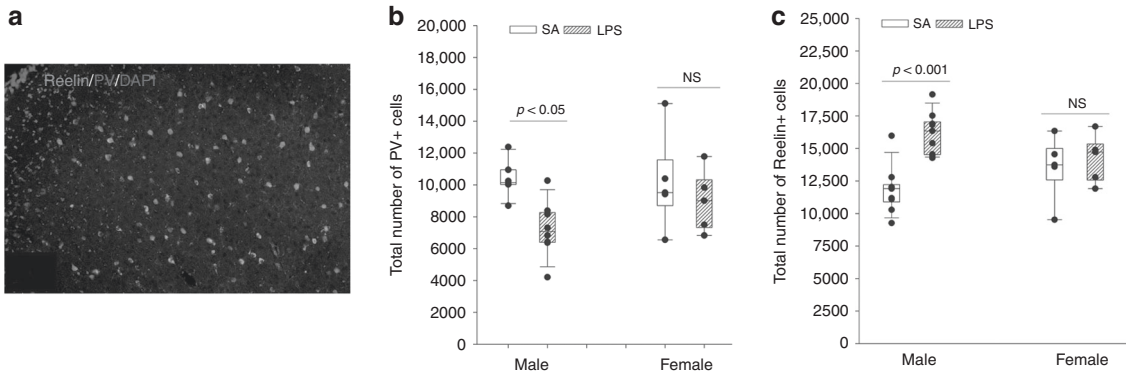

Fig. 5 MIA causes abnormal differentiation of PV+ and Reelin+ interneurons. Representative double immunofluoresence staining of PV+ and Reelin+ neurons in the mPFC of P21 mice offspring (**a**). PV+ and Reelin+ cells were counted in the entire mPFC by stereology. MIA significantly reduced PV+ neurons (**b**) while increased Reelin+ neurons (**c**) in male, but not in female mice offspring. $N = 7$ (male) and 5 (female) per condition.

clear whether this occurs only in a subset of ASD patients linked to maternal infection. In addition, no similar studies have been conducted in younger ASD subjects, e.g., infants around 1 year of age when brain overgrowth is observed.

The role of alternatively activated (M2-like) microglia in abnormal neurodevelopment remains unknown. However, in adult neurological disorders such as multiple sclerosis, Alzheimer's disease,[51] and seizure,[52] they are associated with increased production of anti-inflammatory cytokines and growth/trophic factors such as IGF-1, PDGF, and TGFβ, enhanced microglial phagocytosis, and increased neurogenesis. Even at homeostasis, the adult mouse SVZ harbors a distinct population of M2-like microglia, and depletion of these cells results in a significant decrease in both survival and migration of neuroblasts,[53] suggesting their pro-neurogenic effect. Assuming CD86+/CD206+ developing microglia have similar functional impact on neurons as their adult counterparts, they may stimulate neurogenesis by increasing Ki67+ and Tbr2+ NPCs in the developing brain.

Disruption in excitatory vs inhibitory neurotransmission is a hallmark neuropathology of ASD. Consistent with previous reports,[54,55] we found that MIA leads to a significant reduction of PV+ neurons in the mPFC of male but not female offspring. In contrast, increase in Reelin+ neurons contradicts most reports using MIA models, except the study by Giovanoli et al.[56] who reported increase in Reelin+ neurons in the hippocampus following maternal poly (I:C) exposure. A potential contributing factor for such discrepancy is the age of animals when Reelin+ neurons are assessed. For instance, maternal LPS or poly (I:C) exposure leads to a significant reduction of Reelin+ neurons in the hippocampal stratum orients at P28 but not P14,[57] suggesting that changes of Reelin expression are age-dependent. Other potential contributing factors include variations in gestational age, doses and even serotype of LPS. Clearly, future studies using more standardized animal treatment protocols are needed to address this discrepancy.

Compared to rodents, humans are much heterogeneous in terms of genetic background, environment exposure, and social experience. Thus, the rodent MIA model may capture certain aspects of neuropathological features of ASD, but we should also consider the significant limitation of this model when interpreting research data. Additional limitation of this study is that whether the observed microglia phenotype plays a causative role in abnormal neurogenesis remains unaddressed. Nevertheless, our finding that MIA leads to enhanced neurogenesis may offer mechanistic insight into certain clinical findings in ASD, such as

brain overgrowth. For example, it is possible that a subset of individuals with heightened genetic susceptibility to M2-like microglial response develop abnormal neurogenesis and behaviors upon maternal infection.

In conclusion, our novel findings about unique microglial phenotype and cytokine profiles that are associated with altered neurogenesis and neural differentiation may shed new light on the neurobiological mechanisms of complex NDDs such as ASD.

DATA AVAILABILITY

The datasets generated during and/or analyzed during the current study are available from the corresponding author on reasonable request

REFERENCES

1. Estes, M. L. & McAllister, A. K. Maternal immune activation: implications for neuropsychiatric disorders. *Science* **353**, 772–777 (2016).
2. Bergdolt, L. & Dunaevsky, A. Brain changes in a maternal immune activation model of neurodevelopmental brain disorders. *Prog. Neurobiol.* **175**, 1–19 (2019).
3. Knuesel, I. et al. Maternal immune activation and abnormal brain development across CNS disorders. *Nat. Rev. Neurol.* **10**, 643–660 (2014).
4. Al-Haddad, B. J. S. et al. The fetal origins of mental illness. *Am. J. Obstet. Gynecol.* **221**, 549–562 (2019).
5. Carlezon, W. A. Jr. et al. Maternal and early postnatal immune activation produce sex-specific effects on autism-like behaviors and neuroimmune function in mice. *Sci. Rep.* **9**, 16928 (2019).
6. Haida, O. et al. Sex-dependent behavioral deficits and neuropathology in a maternal immune activation model of autism. *Transl. Psychiatry* **9**, 124 (2019).
7. Fernandez de Cossio, L., Guzman, A., van der Veldt, S. & Luheshi, G. N. Prenatal infection leads to ASD-like behavior and altered synaptic pruning in the mouse offspring. *Brain Behav. Immun.* **63**, 88–98 (2017).
8. Smolders, S., Notter, T., Smolders, S. M. T., Rigo, J. M. & Brone, B. Controversies and prospects about microglia in maternal immune activation models for neurodevelopmental disorders. *Brain Behav. Immun.* **73**, 51–65 (2018).
9. Gilbert, J. & Man, H. Y. Fundamental elements in autism: from neurogenesis and neurite growth to synaptic plasticity. *Front. Cell. Neurosci.* **11**, 359 (2017).
10. Packer, A. Neocortical neurogenesis and the etiology of autism spectrum disorder. *Neurosci. Biobehav. Rev.* **64**, 185–195 (2016).
11. Courchesne, E. et al. Neuron number and size in prefrontal cortex of children with autism. *JAMA* **306**, 2001–2010 (2011).
12. Stoner, R. et al. Patches of disorganization in the neocortex of children with autism. *N. Engl. J. Med.* **370**, 1209–1219 (2014).
13. Courchesne, E. & Pierce, K. Brain overgrowth in autism during a critical time in development: implications for frontal pyramidal neuron and interneuron development and connectivity. *Int. J. Dev. Neurosci.* **23**, 153–170 (2005).
14. Courchesne, E. Brain development in autism: early overgrowth followed by premature arrest of growth. *Ment. Retard. Dev. Disabil. Res. Rev.* **10**, 106–111 (2004).
15. Marchetto, M. C. et al. Altered proliferation and networks in neural cells derived from idiopathic autistic individuals. *Mol. Psychiatry* **22**, 820–835 (2017).
16. Baines, K. J. et al. Maternal immune activation alters fetal brain development and enhances proliferation of neural precursor cells in rats. *Front. Immunol.* **11**, 1145 (2020).
17. Le Belle, J. E. et al. Maternal inflammation contributes to brain overgrowth and autism-associated behaviors through altered redox signaling in stem and progenitor cells. *Stem Cell Rep.* **3**, 725–734 (2014).
18. Ma, Y., Wang, J., Wang, Y. & Yang, G. Y. The biphasic function of microglia in ischemic stroke. *Prog. Neurobiol.* **157**, 247–272 (2017).
19. Loane, D. J. & Kumar, A. Microglia in the TBI brain: the good, the bad, and the dysregulated. *Exp. Neurol.* **275**, 316–327 (2016).
20. Pang, Y. et al. Intranasal insulin protects against substantia nigra dopaminergic neuronal loss and alleviates motor deficits induced by 6-OHDA in rats. *Neuroscience* **318**, 157–165 (2016).
21. Bloem, B. et al. Topographic mapping between basal forebrain cholinergic neurons and the medial prefrontal cortex in mice. *J. Neurosci.* **34**, 16234–16246 (2014).
22. Takagi, S., Furube, E., Nakano, Y., Morita, M. & Miyata, S. Microglia are continuously activated in the circumventricular organs of mouse brain. *J. Neuroimmunol.* **331**, 74–86 (2019).
23. Kokona, D., Ebneter, A., Escher, P. & Zinkernagel, M. S. Colony-stimulating factor 1 receptor inhibition prevents disruption of the blood-retina barrier during chronic inflammation. *J. Neuroinflammation* **15**, 340 (2018).
24. Canetta, S. et al. Maternal immune activation leads to selective functional deficits in offspring parvalbumin interneurons. *Mol. Psychiatry* **21**, 956–968 (2016).
25. Cai, Z., Pan, Z. L., Pang, Y., Evans, O. B. & Rhodes, P. G. Cytokine induction in fetal rat brains and brain injury in neonatal rats after maternal lipopolysaccharide administration. *Pediatr. Res.* **47**, 64–72 (2000).
26. Chua, J. S., Cowley, C. J., Manavis, J., Rofe, A. M. & Coyle, P. Prenatal exposure to lipopolysaccharide results in neurodevelopmental damage that is ameliorated by zinc in mice. *Brain Behav. Immun.* **26**, 326–336 (2012).
27. Cunningham, C. L., Martinez-Cerdeno, V. & Noctor, S. C. Microglia regulate the number of neural precursor cells in the developing cerebral cortex. *J. Neurosci.* **33**, 4216–4233 (2013).
28. Hsueh, P. T. et al. Expression of cerebral serotonin related to anxiety-like behaviors in C57bl/6 offspring induced by repeated subcutaneous prenatal exposure to low-dose lipopolysaccharide. *PLoS ONE* **12**, e0179970 (2017).
29. O'Loughlin, E., Pakan, J. M. P., Yilmazer-Hanke, D. & McDermott, K. W. Acute in utero exposure to lipopolysaccharide induces inflammation in the pre- and postnatal brain and alters the glial cytoarchitecture in the developing amygdala. *J. Neuroinflammation* **14**, 212 (2017).
30. Hu, X. et al. Microglia/macrophage polarization dynamics reveal novel mechanism of injury expansion after focal cerebral ischemia. *Stroke* **43**, 3063–3070 (2012).
31. Thored, P. et al. Long-term accumulation of microglia with proneurogenic phenotype concomitant with persistent neurogenesis in adult subventricular zone after stroke. *Glia* **57**, 835–849 (2009).
32. Ohgidani, M. et al. Microglial Cd206 gene has potential as a state marker of bipolar disorder. *Front. Immunol.* **7**, 676 (2016).
33. Grajchen, E. et al. Cd36-mediated uptake of myelin debris by macrophages and microglia reduces neuroinflammation. *J. Neuroinflammation* **17**, 224 (2020).
34. Hendrickx, D. A. et al. Selective upregulation of scavenger receptors in and around demyelinating areas in multiple sclerosis. *J. Neuropathol. Exp. Neurol.* **72**, 106–118 (2013).
35. Xie, Y. et al. Biglycan regulates neuroinflammation by promoting M1 microglial activation in early brain injury after experimental subarachnoid hemorrhage. *J. Neurochem* **152**, 368–380 (2020).
36. Duan, W., Zou, J., Chen, X., Xiao, C. & Jiang, W. Biglycan expression promotes beta-amyloid-induced microglial activation via TLR2 in mouse cell culture model. *Clin. Lab.* https://doi.org/10.7754/Clin.Lab.2020.200252 (2021).
37. Li, Y. et al. Osteopontin is a blood biomarker for microglial activation and brain injury in experimental hypoxic-ischemic encephalopathy. *eNeuro* https://doi.org/10.1523/ENEURO.0253-16.2016 (2017).
38. Rentsendorj, A. et al. A novel role for osteopontin in macrophage-mediated amyloid-beta clearance in Alzheimer's models. *Brain Behav. Immun.* **67**, 163–180 (2018).
39. De Simone, R. et al. The costimulatory molecule B7 is expressed on human microglia in culture and in multiple sclerosis acute lesions. *J. Neuropathol. Exp. Neurol.* **54**, 175–187 (1995).
40. Wong, H. & Hoeffer, C. Maternal IL-17a in autism. *Exp. Neurol.* **299**, 228–240 (2018).
41. Choi, G. B. et al. The maternal interleukin-17a pathway in mice promotes autism-like phenotypes in offspring. *Science* **351**, 933–939 (2016).
42. Pang, Y. et al. Early postnatal lipopolysaccharide exposure leads to enhanced neurogenesis and impaired communicative functions in rats. *PLoS ONE* **11**, e0164403 (2016).
43. Garay, P. A., Hsiao, E. Y., Patterson, P. H. & McAllister, A. K. Maternal immune activation causes age- and region-specific changes in brain cytokines in offspring throughout development. *Brain Behav. Immun.* **31**, 54–68 (2013).
44. Gupta, S. et al. Transcriptome analysis reveals dysregulation of innate immune response genes and neuronal activity-dependent genes in autism. *Nat. Commun.* **5**, 5748 (2014).
45. Estes, M. L. & McAllister, A. K. Immune mediators in the brain and peripheral tissues in autism spectrum disorder. *Nat. Rev. Neurosci.* **16**, 469–486 (2015).
46. Cui, K., Ashdown, H., Luheshi, G. N. & Boksa, P. Effects of prenatal immune activation on hippocampal neurogenesis in the rat. *Schizophr. Res.* **113**, 288–297 (2009).
47. Hester, M. S., Tulina, N., Brown, A., Barila, G. & Elovitz, M. A. Intrauterine inflammation reduces postnatal neurogenesis in the hippocampal subgranular zone and leads to accumulation of hilar ectopic granule cells. *Brain Res.* **1685**, 51–59 (2018).
48. Lin, Y. L. & Wang, S. Prenatal lipopolysaccharide exposure increases depression-like behaviors and reduces hippocampal neurogenesis in adult rats. *Behav. Brain Res.* **259**, 24–34 (2014).
49. Depino, A. M. Early prenatal exposure to lps results in anxiety- and depression-related behaviors in adulthood. *Neuroscience* **299**, 56–65 (2015).
50. Tsukada, T., Sakata-Haga, H., Shimada, H., Shoji, H. & Hatta, T. Mid-pregnancy maternal immune activation increases Pax6-positive and Tbr2-positive neural

progenitor cells and causes integrated stress response in the fetal brain in a mouse model of maternal viral infection. *IBRO Neurosci. Rep.* **11**, 73–80 (2021).
51. Cherry, J. D., Olschowka, J. A. & O'Banion, M. K. Neuroinflammation and M2 microglia: the good, the bad, and the inflamed. *J. Neuroinflammation* **11**, 98 (2014).
52. Hu, X. et al. Microglial and macrophage polarization-new prospects for brain repair. *Nat. Rev. Neurol.* **11**, 56–64 (2015).
53. Ribeiro Xavier, A. L., Kress, B. T., Goldman, S. A., Lacerda de Menezes, J. R. & Nedergaard, M. A distinct population of microglia supports adult neurogenesis in the subventricular zone. *J. Neurosci.* **35**, 11848–11861 (2015).
54. Wischhof, L., Irrsack, E., Osorio, C. & Koch, M. Prenatal LPS-exposure–a neurodevelopmental rat model of schizophrenia–differentially affects cognitive functions, myelination and parvalbumin expression in male and female offspring. *Prog. Neuropsychopharmacol. Biol. Psychiatry* **57**, 17–30 (2015).
55. Basta-Kaim, A. et al. Prenatal administration of lipopolysaccharide induces sex-dependent changes in glutamic acid decarboxylase and parvalbumin in the adult rat brain. *Neuroscience* **287**, 78–92 (2015).
56. Giovanoli, S., Weber, L. & Meyer, U. Single and combined effects of prenatal immune activation and peripubertal stress on Parvalbumin and Reelin expression in the hippocampal formation. *Brain Behav. Immun.* **40**, 48–54 (2014).
57. Harvey, L. & Boksa, P. A stereological comparison of Gad67 and Reelin expression in the hippocampal stratum oriens of offspring from two mouse models of maternal inflammation during pregnancy. *Neuropharmacology* **62**, 1767–1776 (2012).

ACKNOWLEDGEMENTS

Flow cytometry experiments were performed at the UMMC Cancer Center and Research Institute Flow Cytometry Core Facility, which is supported in part through the UMMC Mississippi Center of Excellence in Perinatal Research (MS-CEPR)-COBRE (P20GM121334). We would like to thank Dr. Ava Bengten, Dr. Melanie Wilson, and Dr. Jon Person for their advice and technical assistance in FACS experiments. Research reported in this publication was supported by the National Institute of General Medical Sciences of the National Institutes of Health under Award Number P20GM121334. The content is solely the responsibility of the authors and does not necessarily represent the official views of the National Institutes of Health.

AUTHOR CONTRIBUTIONS

Y.P. and A.B. conceived the study. M.L., A.B., and Y.P. contributed to the study design and drafted the manuscript. M.L., S.L., K.C., S.R., and Y.P. performed experiments. M.L., N.O., L.-W.F., and Y.P. contributed to data analysis.

COMPETING INTERESTS

The authors declare no competing interests.

ADDITIONAL INFORMATION

Supplementary information The online version contains supplementary material available at https://doi.org/10.1038/s41390-022-02239-w.

Correspondence and requests for materials should be addressed to Abhay Bhatt or Yi Pang.